Characterizing Electrical Arc Behavior in Ion Engines

Robert E. Thomas
NASA Glenn Research Center, Cleveland, OH, 44135, USA

Rittu S. Raju
HX5, LLC, Cleveland OH, 44135, USA

James J. Bontempo
ZIN Technologies, Cleveland, OH, 44130, USA

Test results using an engineering model Advanced NEXT thruster are presented to identify different arc types utilizing ground test hardware. Three distinct arc types were observed: grid-to-grid arcs, high voltage-to-chassis arcs, and a combination of both. The frequency of high voltage-to-chassis arcs ranged from 4-30%, depending on operating conditions and hardware configuration. Higher beam currents were typically associated with more frequent high voltage-to-chassis arcs. During these arcs, the measured chassis current levels ranged from 20-70 A, however a significant portion of the output beam current returned to the beam supply via the neutralizer cathode plasma, which may be a ground test facility effect. The paper also discusses conducted susceptibility tests that can be performed at the spacecraft level to address the transients associated with arcing events.

I. Nomenclature

J_a = accelerator grid current, A
J_b = beam current (= $J_{bps} - J_a$), A
J_{bps} = beam power supply current, A
J_g = ground current, A
V_a = accelerator grid voltage, V
V_{bps} = beam power supply voltage, V
V_g = coupling voltage, V

II. Introduction

Gridded ion engines represent a class of electric thrusters characterized by high propulsive efficiency and high total impulse capabilities. These engines operate by applying high voltage to multi-aperture electrodes, electrostatically accelerating ions to generate thrust. High voltage breakdowns periodically occur within the thruster during the course of normal operations. These breakdowns, or arcs, constitute an inherent aspect of operation, with observations indicating a diminishing frequency over the thruster's on-orbit operational lifespan. To safeguard the propulsion system during such occurrences, the power processing unit (PPU) employs an automated arc extinction sequence, termed "recycle," which is triggered upon detection of an over-current condition caused by a breakdown [1]. The initial phase of this sequence involves momentarily deactivating the high voltage and reducing the discharge current to a predetermined level. The high voltage is subsequently reapplied, and the discharge current is returned to its nominal value. The electrical breakdown that triggers the sequence typically lasts for hundreds of microseconds, while the recycle sequence itself is approximately 800 milliseconds for the NEXT-C system.

During operation, the thruster may encounter different types of high-voltage arcs. The most common of these occur between the screen and accelerator electrodes, followed by arcs between high-voltage surfaces and the thruster chassis. While the arcs that triggers the recycle sequence may provide information regarding potential hardware issues, such as insulator failures, both the thruster and PPU are designed to withstand such occurrences. As such, the specific nature of recycle events during typical ground operations has not been extensively characterized. Reevaluation of data

collection methods has been prompted by a spacecraft anomaly encountered during the Double Asteroid Redirection (DART) mission, as summarized below.

The DART mission, NASA's inaugural mission from the Planetary Defense Coordination Office, aimed to kinetically deflect a small asteroid and measure its resultant trajectory perturbation [2]. The spacecraft launched on Nov. 24, 2021, and successfully intercepted Dimorphos on Sept. 26, 2022. The DART mission served as technology demonstration platform for multiple technologies, including NASA's Evolutionary Xenon Thruster Commercial (NEXT-C) propulsion system, which was jointly developed by Aerojet Rocketdyne, ZIN Technologies, and the NASA Glenn Research Center [3]. On December 18, 2021, the NEXT-C system underwent its first activation in flight following four days of spacecraft-level checkouts. During its operation, the system experienced 21 recycles over two hours of operation, a result consistent with NSTAR flight data [4]. Subsequent analysis of the spacecraft telemetry revealed an anomaly in the spacecraft's power system electronics (PSE), evidenced by a 50% step increase in current within the Interface-Controller-Low (ICL) voltage power supply. This current step increase was concurrent with a NEXT-C recycle event. A NASA Engineering and Safety Center (NESC) investigation into the anomaly found that a field-programmable gate array (FPGA) I/O pin receiving a signal from the output of a buffer/latch was improperly configured, and it was hypothesized that electromagnetic interference induced by a recycle due to a high voltage-to-chassis arc propagated into the PSE ICL slice [5]. A subsequent CS116 conducted susceptibility test on benchtop PSE engineering hardware reproduced an identical current step increase upon application of common mode injection into the PSE. While the increased ICL current did not disrupt spacecraft operations, it highlighted insufficient thruster/spacecraft electrical testing during pre-launch checkouts, prompting the suspension of further NEXT-C operations. The anomaly investigation also elicited inquiries into the frequency of recycles induced by high-voltage-to-chassis arcs compared to grid-to-grid arcs, and the magnitude of chassis currents. These measurements have historically been uncharacterized during ion engine ground tests and thus represent a knowledge gap in the technical literature.

To bridge this gap, recent ion thruster tests at NASA GRC have incorporated instrumentation to characterize the arc behavior using an Advanced NEXT engine. These tests have been conducted as part of the Advanced NEXT program, a collaborative initiative involving the United States Space Force (USSF), private industry, and NASA [6]. The Advanced NEXT project seeks to build on previous investments in the NEXT design, seeking to make minimal changes to the system architecture to enable operation at higher thrust-to-power levels. This paper will examine the prevalence of different types of arcing events that cause recycles using ground test hardware and identify factors such as input conditions and configurations that may influence the arc type. The discussion will begin with a summary of the throttle levels and hardware configuration used during testing. This will be followed by an explanation of the different types of recycles observed, along with the associated experimental data. The paper will conclude with a review of conducted susceptibility tests that can be performed at the spacecraft level to address transients during recycle events.

III. Operating Conditions

Tests were performed using the throttle table shown in Figure 1, where each throttle level (TL) corresponds to a unique combination of beam current (J_b) and beam power supply voltage (V_{bps}). The green cells represent the "standard" NEXT throttle levels, while the blue cells highlight extended performance conditions relevant to both commercial and military applications. The standard conditions were initially defined based on the needs of planetary science missions and have been extensively characterized [7]. The blue conditions involve operation at high beam current levels, with thrust values reaching up to twice that of the standard throttle levels. These conditions have been investigated experimentally [8-10], and the necessary PPU and thruster modifications to operate under these conditions are outlined in Ref. 6. Data for both operational regimes will be presented in the following sections.

	V_{bps}, V															
J_b, A	1800	1567	1396	1179	1200	1068	1021	936	870	850	700	679	650	400	300	275
7.04	1B-HP	TL55	TL54	TL53			TL52	TL51C	**1B**		TL51A					
6.00					**2B**											
5.80	1A-HP	TL50	TL49	TL48		**1A**		TL46B	TL46A		TL46					
5.50	TL46G	TL45F	TL45E	TL45D			TL45C	TL45B	TL45A		TL45					
5.00	TL44G	TL44F	TL44E	TL44D			TL44C	TL44B	TL44A		TL44		TL44-###			
4.50	TL43G	TL43F	TL43E	TL43D			TL43C	TL43B	TL43A		TL43		TL43-###	TL43-###		
4.00	TL42G	TL42F	TL42E	*TL42D*			TL42C	TL42B	TL42A		TL42		TL42-###			
3.52	TL40	TL39	TL38	TL37			ETL3.52A	ETL3.52B		ETL3.52C	ETL3.52D		TL37-###	TL37-###		
3.10	TL36	TL35	TL34	TL33			ETL3.1A	ETL3.1B		ETL3.1C	ETL3.1D	ETL3.1E		TL33-###		
2.70	TL32	TL31	TL30	TL29			TL28	ETL2.7A		ETL2.7B	ETL2.7C	ETL2.7D	ETL2.7E			
2.35	TL27	TL26	TL25	TL24			TL23	ETL2.35A		ETL2.35B	ETL2.35C	ETL2.35D	TL2.35E			
2.00	TL22	TL21	TL20	TL19			TL18	ETL2.0A		ETL2.0B	ETL2.0C	ETL2.0D	ETL2.0E			
1.60	TL17	TL16	TL15	TL14			TL13	ETL1.6A		ETL1.6B	ETL1.6C	ETL1.6D	ETL1.6E	ETL1.6F		
1.20	TL12	TL11	TL10	TL09			TL08	TL07		TL06		TL05	TL04	TL03	TL02	
1.00																TL01

Figure 1: Throttle table utilized during ground tests.

IV. Test Hardware

A. Ground Support Equipment

Tests were completed in Vacuum Facility 16 (VF16) at NASA GRC. The 2.7 m diameter × 8.5 long facility is evacuated with 10 cryopumps and has a base pressure of 2.0 x 10^{-7} torr. The Xe corrected facility pressure during operation at 3.52 A and 7.04 A of beam current were 2.5 × 10^{-6} torr, and 4.7 × 10^{-6} torr, respectively. A data acquisition system monitored ion engine and facility operation. A high-purity xenon feed system delivered propellant to the discharge cathode, neutralizer cathode, and discharge chamber main plenum through individual mass flow controllers. Thruster and vacuum facility telemetry were written to a data file at a rate of 1 Hz during thruster operation. A full description of the test support equipment can be found in Ref. 11.

A power console consisting of six commercially available power supplies with integrated recycle logic circuitry was used to power the engine and is similar to that described in Ref. 12. A schematic of the power console is shown in Figure 2. The console provides the power required for thruster operation via six separate power supplies. These supplies include the discharge cathode heater, neutralizer cathode heater, discharge, neutralizer keeper, and the high voltages for the screen and accelerator grids. Four of these supplies are needed during steady-state operation, while the heaters (and two igniters) are only required during thruster startup. Several additional circuit elements are incorporated into the system, which are noteworthy for the current study. A Zener diode and capacitor isolate neutralizer common from facility ground during steady-state operation, and these elements provide a current path during transient events, such as recycles. Additionally, a 33 Ω resistor is placed in series with the positive lead of the accelerator grid supply. This resistor affects the current path during recycles and is primarily intended to reduce electrode pitting during recycles by limiting the peak arc current.

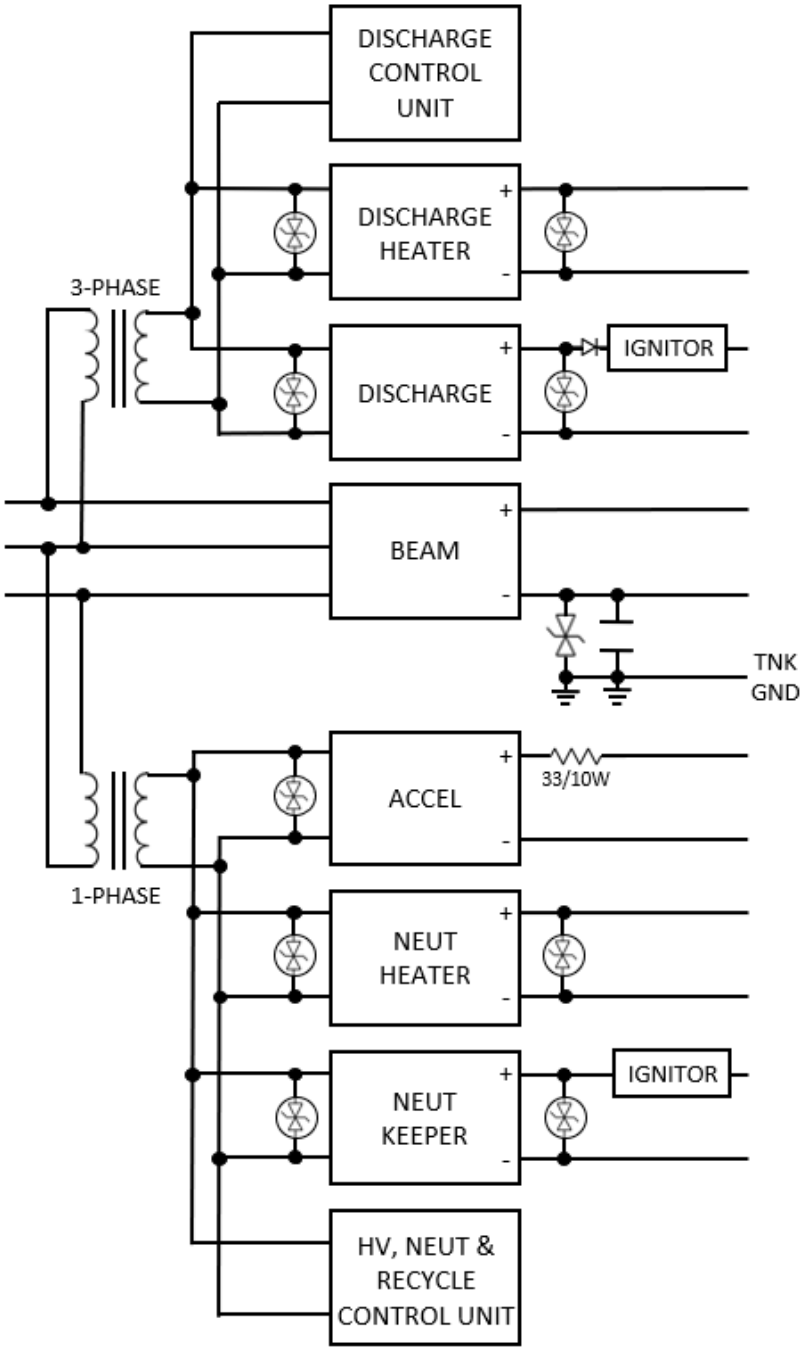

Figure 2: Schematic of the power supplies used during ground testing.

B. Ion Engine

Tests were conducted on an Advanced NEXT ion engine (Fig. 3), which consists primarily of engineering model (EM) subassemblies designed and characterized during the NEXT development program [13]. Two notable hardware modifications were made to the heritage NEXT design to enable stable operation at the high thrust-to-power conditions of interest and are described in detail in Ref. 6. The first modification involved changes to the ion optics geometry. Two different ion optics designs were tested. One design incorporated high-perveance ion optics, which were fabricated with a larger active beam diameter, reduced thickness, and larger apertures compared to the original NEXT optics. Additionally, the pathfinder ion optics from the NEXT-C flight project were also tested. Results for both ion optics configurations are presented. The second modification was the addition of a baffle assembly downstream of the discharge cathode. The baffle acts as a physical barrier to reduce a performance limiting off-axis current density peak. Figure 4 compares the current density profiles with and without the baffle. The current density peak is associated with localized ion impingement on the grids and severely degrades the current extraction capability of the ion optics, particularly at the beam currents of interest for the Advanced NEXT program [10]. The baffle effectively eliminates the current peak, resulting in a substantial reduction in recycle rate as will be shown in a later section.

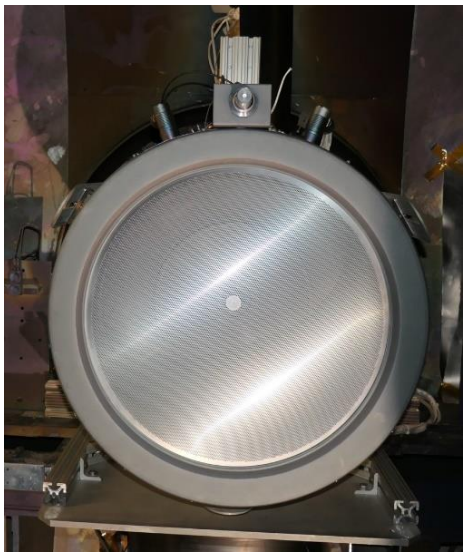

Figure 3: Pretest photograph of EM6.

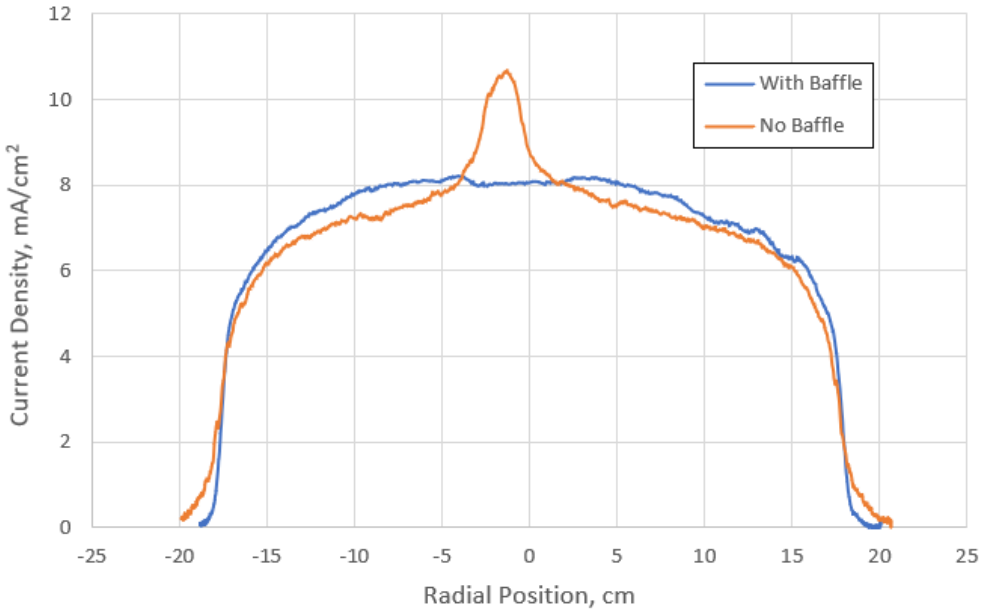

Figure 4: Current density profile obtained 3 cm below centerline at the throttle level AF1B (V_b = 870 V, J_b = 7.04 A) [Ref. 6] .

C. Diagnostics

A series of current and voltage probes were utilized to characterize the arc types. The types of current probes are summarized in Table 1, with their locations within the circuit shown in Figure 5. Three of the current signals were acquired using current transformers, while a Hall effect probe was used to measure both the AC and DC components of the current. The reported chassis currents were measured with the Hall effect probe. The measured parameters were of interest for various reasons. During an arc event, the majority of the arc current is sourced from the beam supply (J_{bps}) output filter, whose capacitors are charged to voltages of up to 1.8 kV during testing. The current from the accelerator grid supply (J_a) provides insight into the current paths during a recycle as well as the impingement current magnitude as the beam is temporarily defocused. Two current probes were placed within the system to monitor the magnitude of the chassis current (J_g). A subset of the initial tests employed voltage probes, although they were later redeployed to measure other thruster parameters in later tests. The accelerator grid voltage (V_a) serves as an indicator for distinguishing between different arc types, including both anode- and accelerator grid-to-chassis arcs. Additionally, the coupling voltage (V_g) has been shown to correlate with the arc type, and this telemetry is integrated into the circuitry for the Advanced NEXT PPU.

Table 1: High speed current telemetry obtained during testing.

	Measurement	Sensor Type	Sensor Output (Volts/Amp)
Channel 1	Beam Supply	Current Transformer	0.1
Channel 2	Accelerator Supply	Current Transformer	0.1
Channel 3	Ground Current	Hall Effect	---
Channel 4	Ground Current	Current Transformer	0.1

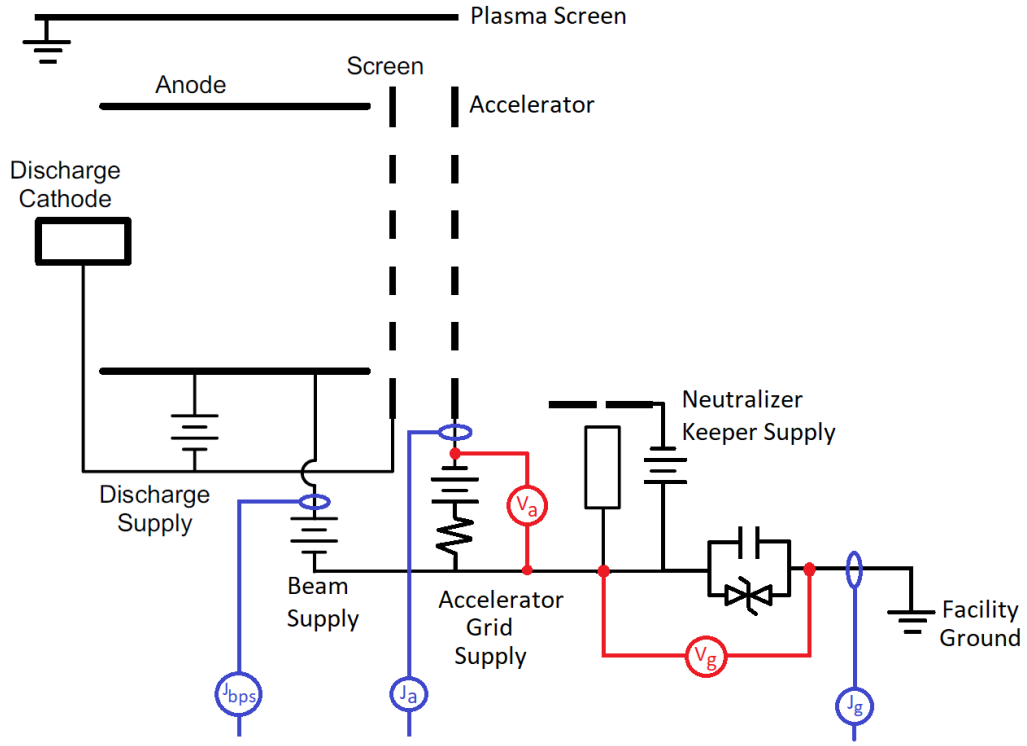

Figure 5: Power supply schematic and location of voltage and current probes.

V. Advanced NEXT vs. NEXT-C Test Differences

The data collected during testing established a baseline for differentiating the various arc types. However, it's important to highlight the hardware and operational differences between the Advanced NEXT test article and the flight engine developed during the NEXT-C project that was flown on the DART mission.

1. To date, all tests in the Advanced NEXT program have been conducted using an engineering model thruster, which has significant design differences compared to the prototype model or flight thruster design. For instance, the EM design lacks the emissivity coatings found on higher-fidelity engines, leading to differences in peak operating temperatures. These temperature differences could influence the grid gap and interelectrode electric field. Additionally, the EM low-voltage propellant isolator (LVPI) design incorporates a high open-area plasma screen, which allows the cathode plasma to arc across the LVPI, creating an additional current path during recycles [14]. A comparison of the engineering and prototype model designs can be found in Ref. 15.
2. The subassemblies for the EM6 engine were manufactured in the mid-2000s, with certain components, such as the hollow cathodes, having been previously tested in other engines. As such, the thruster has undergone significantly more modifications and handling than a typical flight article. Initial tests conducted during the Advanced NEXT project indicated that foreign object debris (FOD) generated during the assembly process could significantly affect both the recycle rate and magnitude of the chassis currents. In contrast, flight hardware would experience far less handling and would be subject to stringent configuration and contamination controls, reducing the likelihood of FOD generation.
3. Ground tests were performed using commercial power supplies with transmission lines several factors longer than those used on the DART spacecraft. While these longer lines allowed for easier hardware modifications in between tests, they also resulted in relatively high line inductances, affecting the impedance distributions throughout the system. Additionally, the inline resistors of the power console were generally higher than those of the PPU, and the output capacitance of the commercial beam supply is an order of magnitude greater than that of the PPU, resulting in increased energy dissipation during arc events. Collectively, these differences affect the circuit behavior of the system, including current paths, time constants, and peak amplitudes, although the precise impacts of these differences have not been quantified through modeling.
4. The high thrust-to-power conditions of interest for the Advanced NEXT project involved both elevated discharge powers and beam currents compared to the standard NEXT throttle table. The discharge powers were up to twice as high, potentially resulting in a reduced grid gap and increased electric field between the electrodes. Finally, at elevated beam currents, the off-axis current density peak became more pronounced, significantly affecting the perveance margin and recycle rates as detailed in Ref. 10.

VI. Arc Types

The electrical breakdowns within the thruster may be caused, in part, by thermal desorption of adsorbed gases, FOD, sharp edges, and/or localized steering of charged particle beams. Three distinct arc types have been identified and are described below.

1. **Grid-to-grid arcs**: These arcs occur between the screen and accelerator grids and prior to testing were anticipated to be the most common, due to sub-millimeter interelectrode gaps, potential differences of up to 2 kV, and charged particles traversing the gap during thruster operation. Two arc electron current return paths are illustrated in Figure 6. During a grid-to-grid arc, the beam supply is shorted across the accelerator grid, allowing the current to travel across the high-voltage supplies and return to cathode common or the screen grid (not shown in Fig. 6) via the discharge plasma. A series of diodes and voltage suppressors (not shown) used to protect the power supplies allow current along Path 1. During a grid-to-grid recycle, the accelerator grid potential is driven towards the beam potential (Figure 7), which can induce electron current from the neutralizer due to its higher potential, providing the second current path. While these represent the two primary current paths, the actual current flow is distributed throughout the system, as evidenced by the oscilloscope traces in Figure 8. The grid-to-grid arcs were characterized by relatively short time scales (due to a small RC time constant), and generally exhibited low chassis current amplitudes. While the peak currents from the beam supply output filter could exceed 100 A during these arcs, the measured chassis currents were typically in the range of 5-10 A. Although the coupling voltage can potentially indicate the arc type, the data collected using the high-voltage probe in Figure 7 exhibited significant noise, preventing effective arc discrimination. It is

possible that the output filtering within the PPU may yield a more discernible signal, which will be evaluated in future system integration tests.

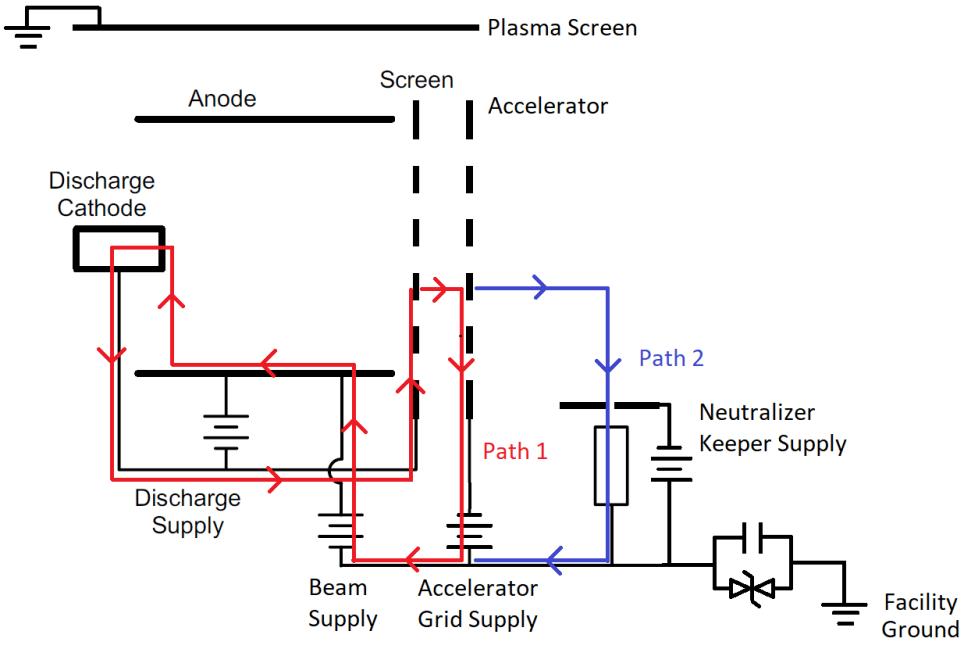

Figure 6: Current paths during a grid-to-grid arc.

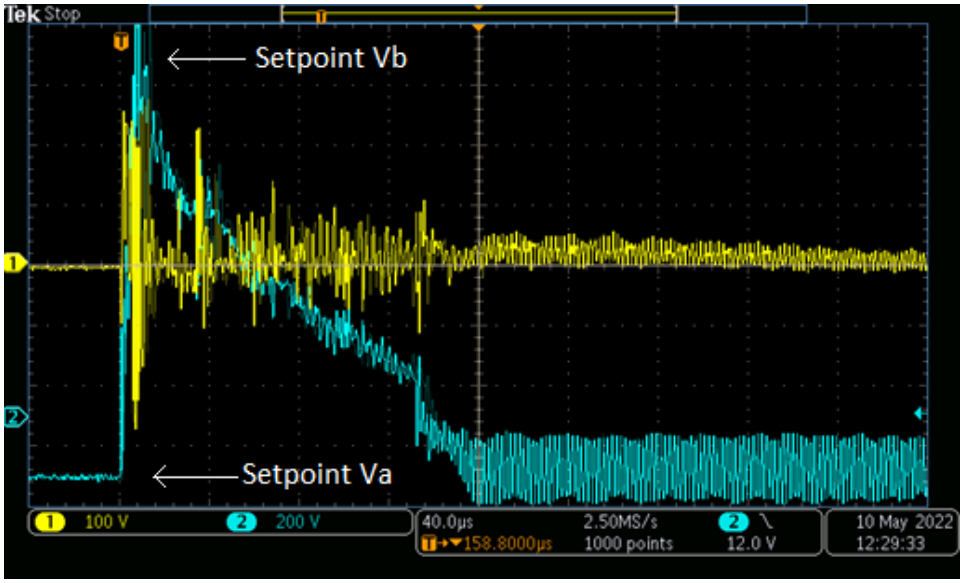

Figure 7: Coupling voltage (Ch 1) and accelerator grid voltage (Ch 2) during a grid-to-grid recycle at TL19 (V_b = 1179 V, J_b = 2.00 A).

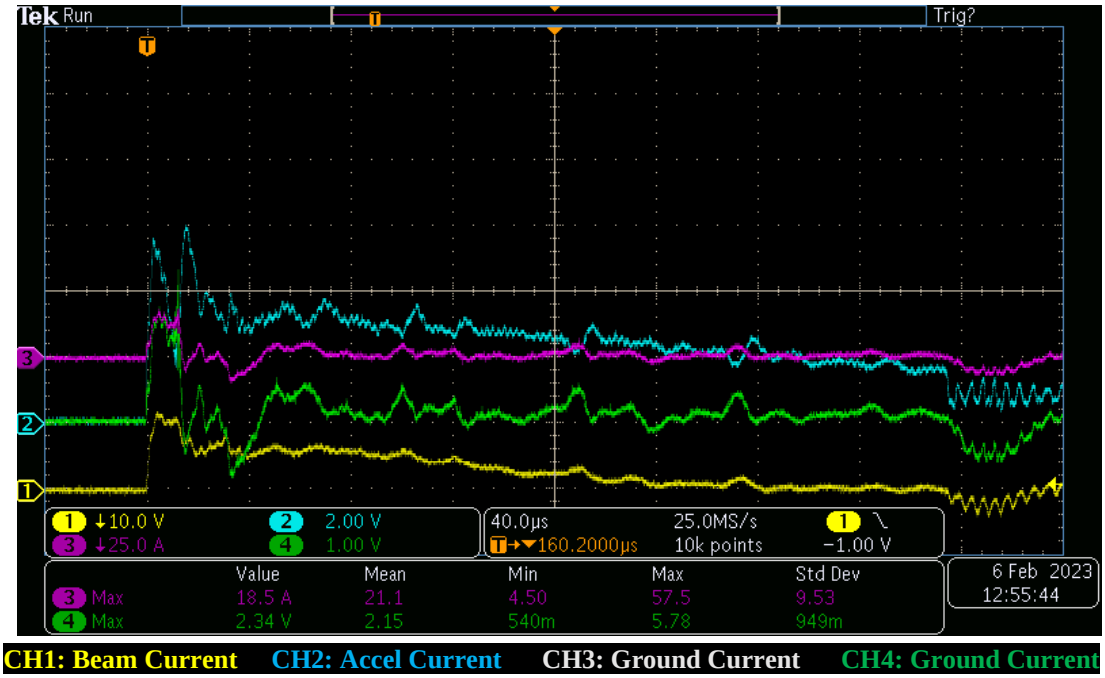

Figure 8: Current probe oscilloscope trace obtained during a high voltage-to-chassis arc at throttle level AF1A (V_b = 1068 V, J_b = 5.80).

2. **HV-to-chassis arcs**: These arc types occur between high-voltage surfaces and chassis (facility ground) potential surfaces. The high-potential surfaces include the anode and cathode potential surfaces, while the chassis potential surfaces include the plasma screen, the low side of the propellant isolators, and the thruster mounting structure. Although the precise arcing locations during thruster operation cannot be ascertained, anode-to-chassis arcs are considered the most likely due to the relatively large exposed surface area. Accelerator grid to chassis arcs are also possible, though considered less likely, due to the lower potential differences (< 350 V) and the larger physical gaps involved. Figure 9 illustrates two potential current paths for both anode-to-chassis and cathode-to-chassis arcs (the potential difference between anode and cathode is approximately 30 V). In these scenarios, the current arcs to a grounded surface (e.g., plasma shield) and completes the circuit through neutralizer common. During testing, it was observed that approximately 10-20% of the output beam supply current flowed through path 1, while the remaining current followed path 2. This current distribution may be a consequence of the ground testing conditions. Path 2 arises from the neutralizer cathode being driven negative with respect to the facility ground during the arc. In ground tests, the neutralizer cathode is surrounded by the grounded facility, which provides a low-impedance path due to the exposed surfaces of the facility. During flight, the spacecraft chassis will act as the ground, and the available exposed surfaces will be more limited. The current traces from a high voltage-to-chassis arc differs from grid-to-grid arc, as depicted by the traces shown in Figure 10. The peak beam supply current was generally several factors higher during a high voltage-to-chassis arc, indicating a lower impedance path, and the pulse period was also several times longer.

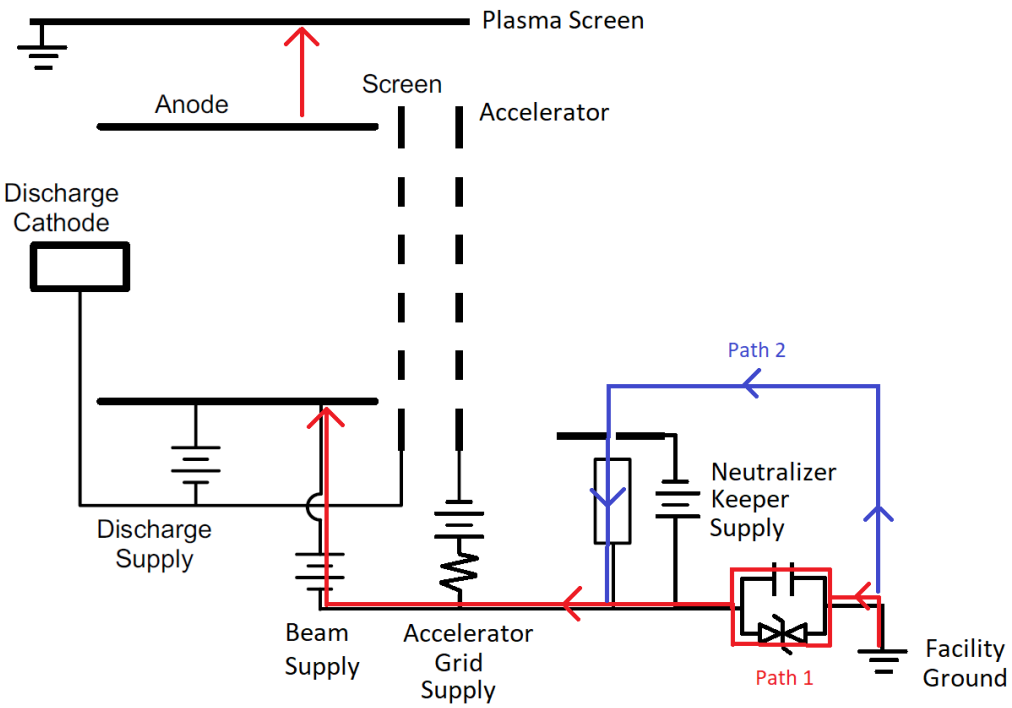

(a)

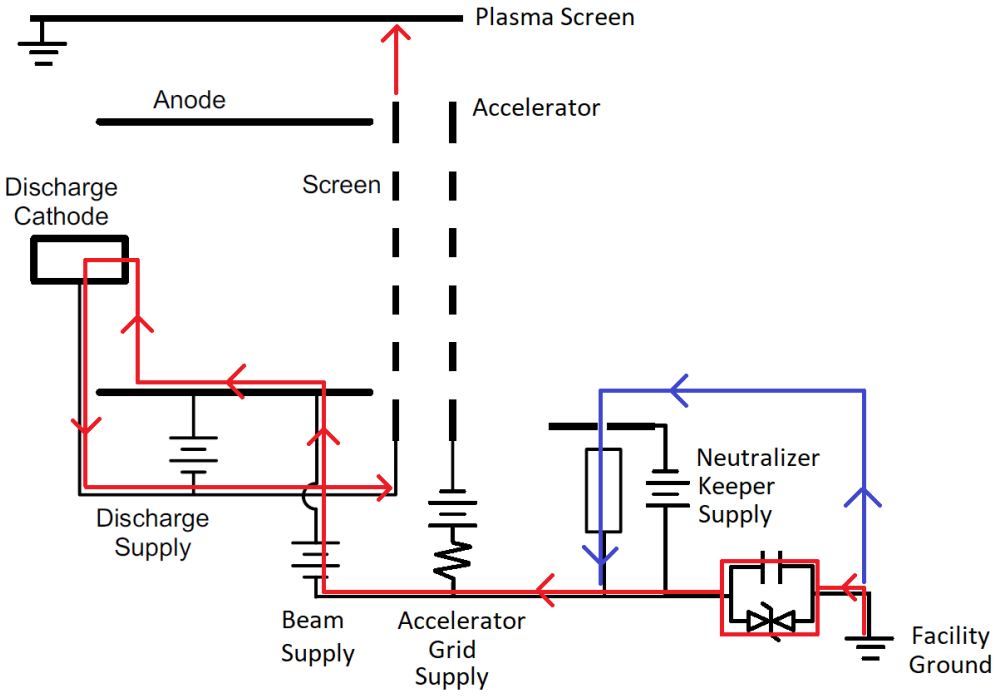

(b)

Figure 9: Current paths during an (a) anode and (b) cathode to high voltage-to-chassis arc.

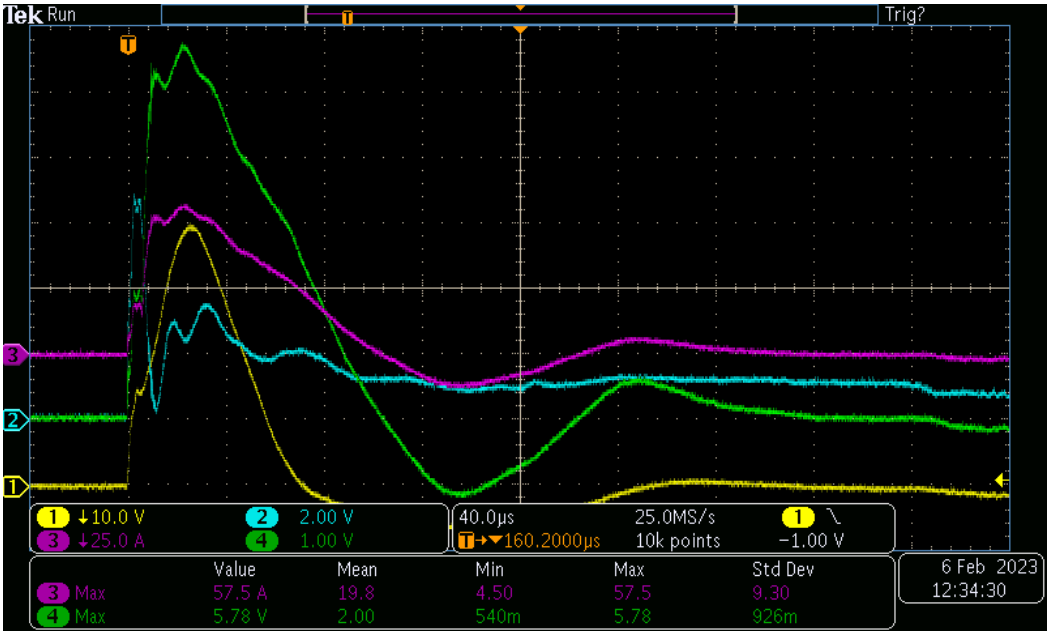

CH1: Beam Current **CH2: Accel Current** **CH3: Ground Current** **CH4: Ground Current**

Figure 10: Current probe oscilloscope trace obtained during a high voltage-to-chassis recycle at throttle level AF1A (V_b = 1068 V, J_b = 5.80).

3. **Combined arcs**: This arc type is a combination of the two aforementioned arcs, as shown in Figure 11. In this sequence, a grid-to-grid arc typically initiates the recycle process, followed closely by a high voltage-to-chassis arc. As will be detailed in a later section, these types of recycles accounted for a relatively small proportion of the total recycles at the standard throttle conditions but were slightly more prevalent at elevated beam currents.

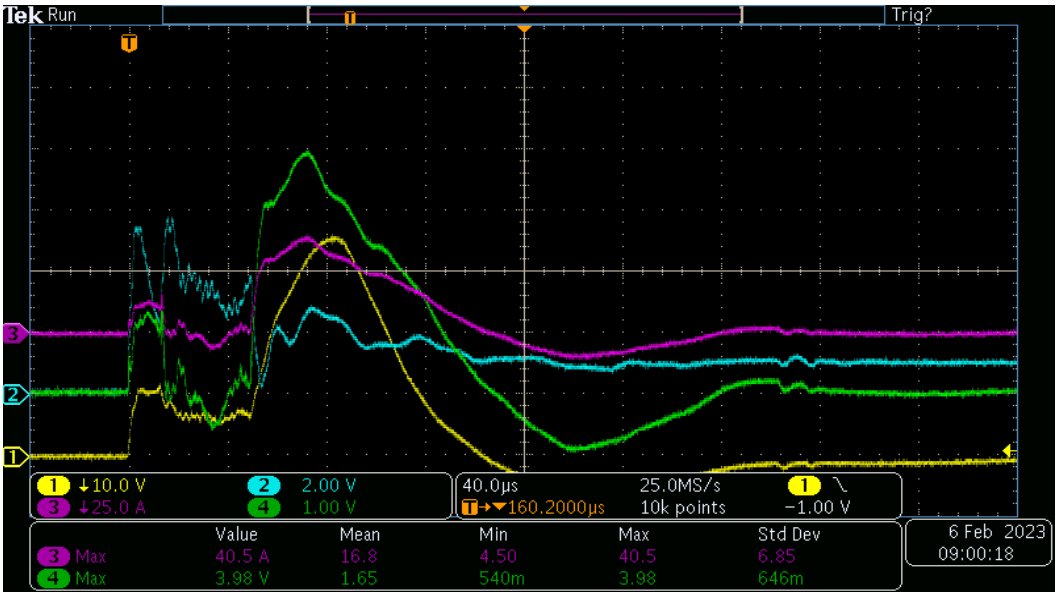

CH1: Beam Current **CH2: Accel Current** **CH3: Ground Current** **CH4: Ground Current**

Figure 11: Current probe oscilloscope trace obtained during a combined arc recycle at ETL3.52C (V_b = 850 V, J_b = 3.52 A).

VII. Test Results

A series of tests were conducted and are listed in Table 2. The tests are categorized based on the thruster configuration. Test Segment 1 employed the heritage EM NEXT design with the high perveance ion optic design. Test Segment 2 utilized the high perveance optics and marked the first instance of employing a baffle assembly to allow for operation at the desired Advanced NEXT throttle levels. Test Segment 3 was comprised of several tests that utilized the heritage NEXT-C ion optics design with minor changes to the baffle geometry. The following subsections summarize the test results for both the standard NEXT throttle table conditions ($J_b \leq 3.52$ A) and the high thrust-to-power conditions ($J_b > 3.52$ A) for the different hardware configurations.

Table 2: Ion optics and baffle configuration for the different test segments.

Test Segment	Ion Optics Assembly	Baffle?
#1	High Perveance Design	No baffle
#2	High Perveance Design	With baffle
#3	Heritage NEXT-C Design	With baffle

Test Segment 1

The recycle rate at standard throttle levels averaged one or fewer recycles per hour during steady-state operation, consistent with previous ground test data, and is shown in Figure 12. The anomalous rate of 10 recycles per hour observed on the first day of testing was primarily attributed to the rapid power ramp-up following exposure to the atmosphere. Approximately 90% of the recycles within the standard throttle table were due to grid-to-grid arcs. At higher beam current levels, the recycling behavior was dominated by the off-center current density peak. This peak resulted in direct ion impingement on the grids, causing an order of magnitude increase in the recycle rate, as shown in Figure 13. Visual observations during testing confirmed grid-to-grid arcing consistently occurring at the location of peak current density, which was corroborated by post-test grid inspections. While chassis currents for high voltage-to-chassis arcs were not captured at the standard throttle conditions (Figure 14), they were in the range of 30-60 A at the elevated beam current conditions, as shown in Figure 15. The percentage of recycles due to grid-to-grid arcs slightly declined from 90% to 84% at the higher beam current levels. Subsequent tests employed a baffle to mitigate the off-center peak and reduce the recycling rate, particularly at the desired high thrust-to-power conditions.

Test Segment 2

The introduction of a baffle did not significantly affect the recycling behavior of the engine at the standard throttle levels. However, the baffle had a notable impact at high thrust-to-power conditions due to the elimination of the current density peak. During the initial phase of testing, at elevated beam currents, the recycling rate was relatively high (>10 per hour), likely due to the throttling profile used in combination with potential gas desorption at high power levels. Over time, the recycling rate decreased and stabilized at approximately 2-3 per hour towards the end of the test. Nearly all of the recycles at the standard throttle levels were due to grid-to-grid arcs (96%), while this percentage dropped to 70% under high thrust-to-power conditions. Peak chassis currents for high voltage-to-chassis arcs ranged from 25 to 50 A across both operational regimes. Subsequent tests utilized a baffle assembly while reverting to the NEXT-C ion optic design, in part, to preserve the flight-qualified heritage NEXT-C design where feasible.

Test Segment 3

This series of tests utilized the most mature thruster configuration to date for the Advanced NEXT program. The recycle rate was generally low across all conditions, with tens of hours sometimes elapsing in between recycle events. The proportion of recycles due to high voltage-to-chassis arcs was 81% and 70% under standard and high thrust-to-power conditions, respectively. The low recycle rate observed during these tests resulted in a much smaller sample size compared to previous tests, which may have impacted the results. Nevertheless, the general trend of a higher percentage of high voltage-to-chassis arcs at elevated beam currents was observed. As in prior tests, chassis currents for high voltage-to-chassis arcs ranged from 20 to 70 A. A summary of the different arc types is shown in Figures 16 and 17.

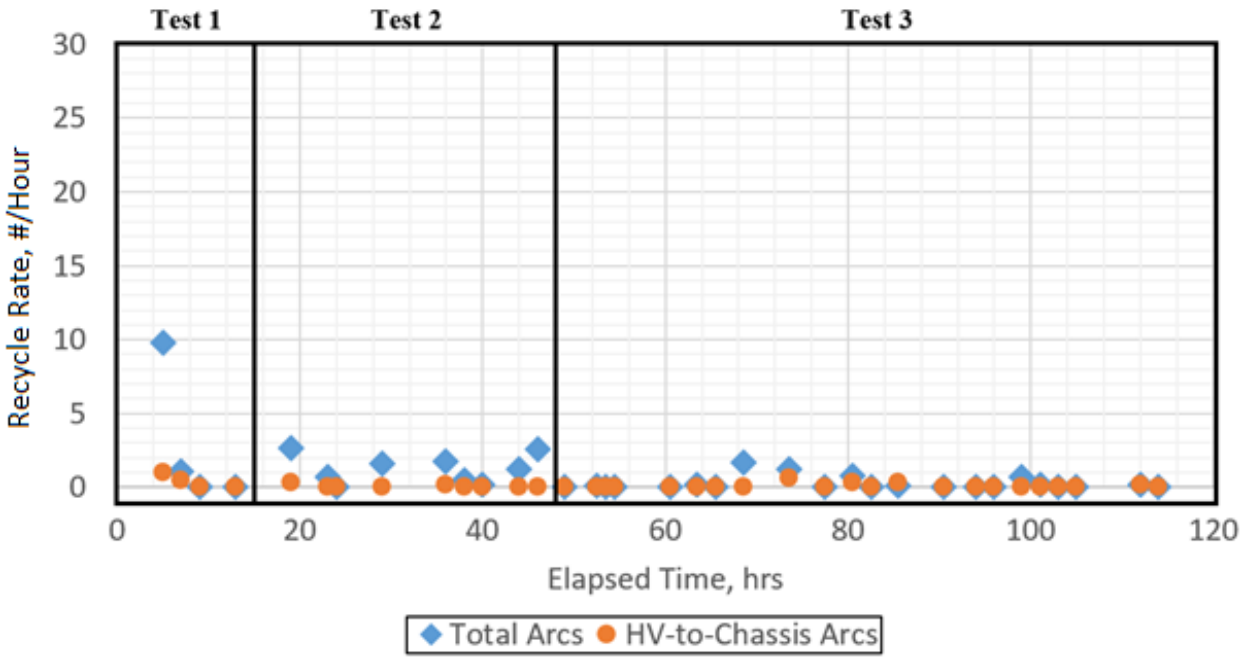

Figure 12: Recycle rate at the standard throttle table conditions.

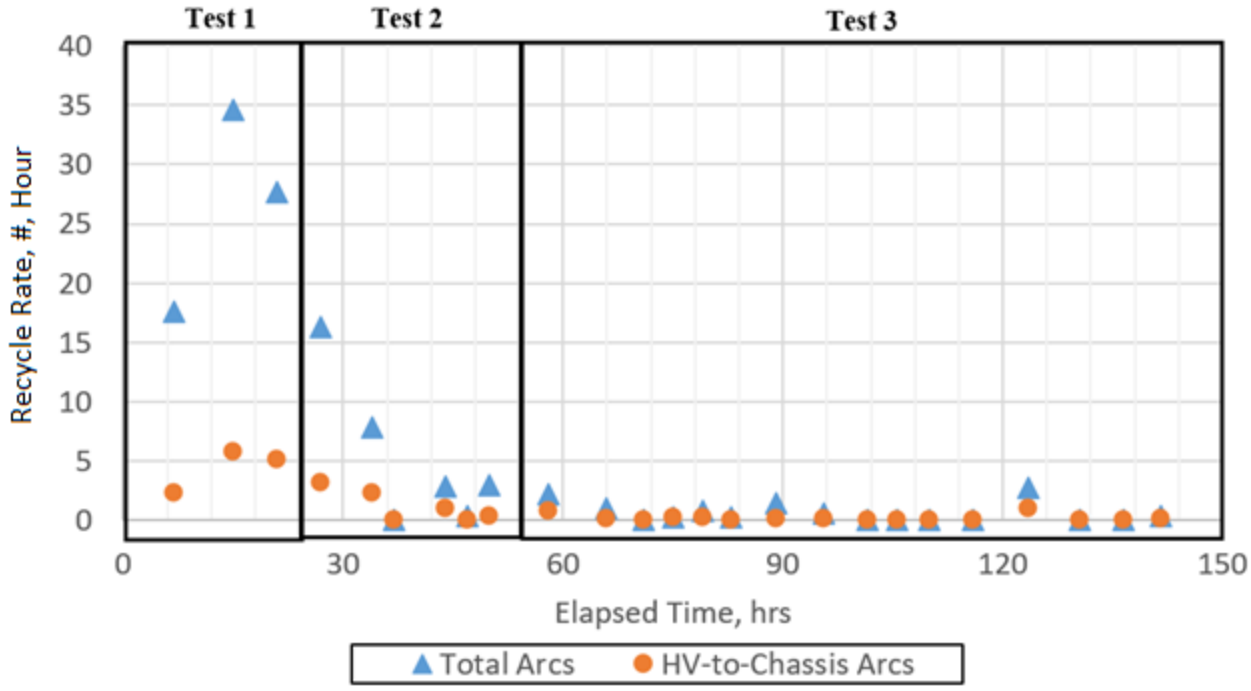

Figure 13: Recycle rate at the high thrust-to-power conditions.

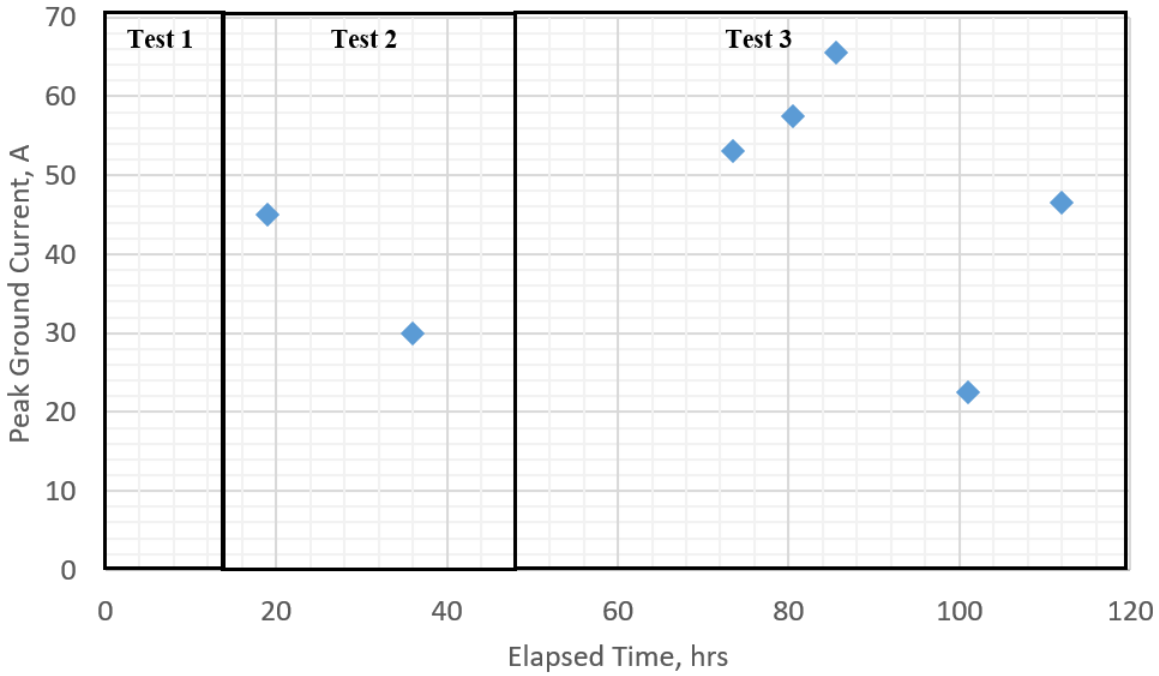

Figure 14: Peak chassis currents during high voltage-to-chassis arcs at the standard throttle conditions.

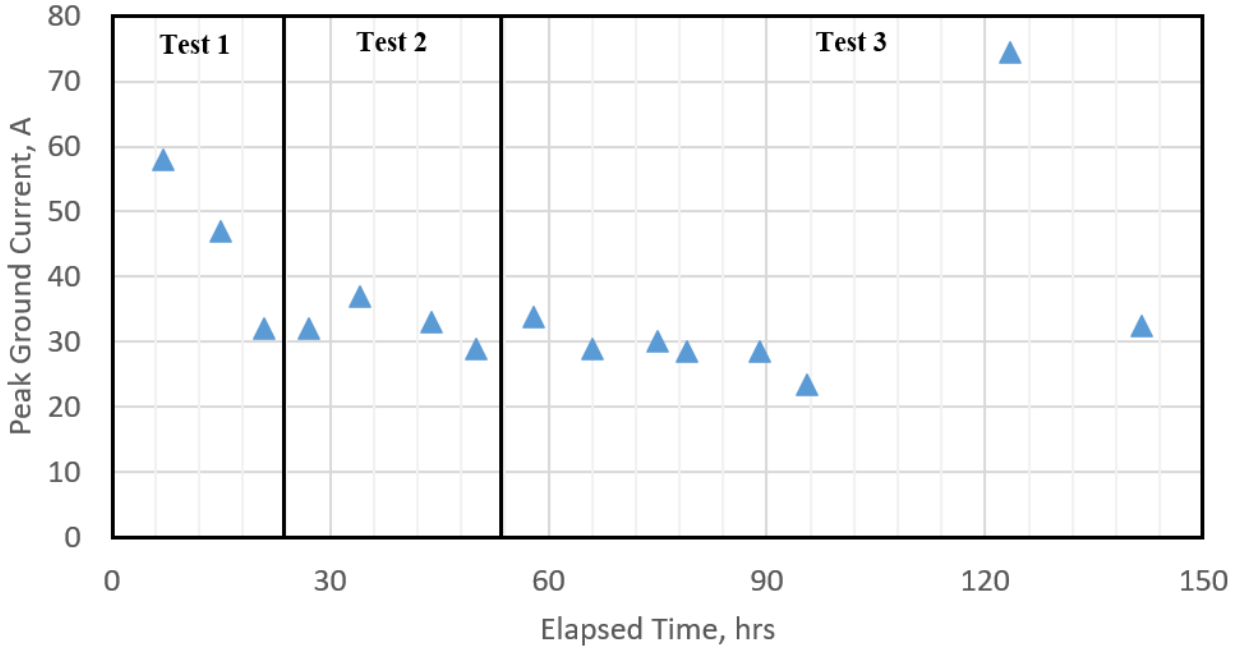

Figure 15: Peak chassis currents during high voltage-to-chassis at the high thrust-to-power conditions.

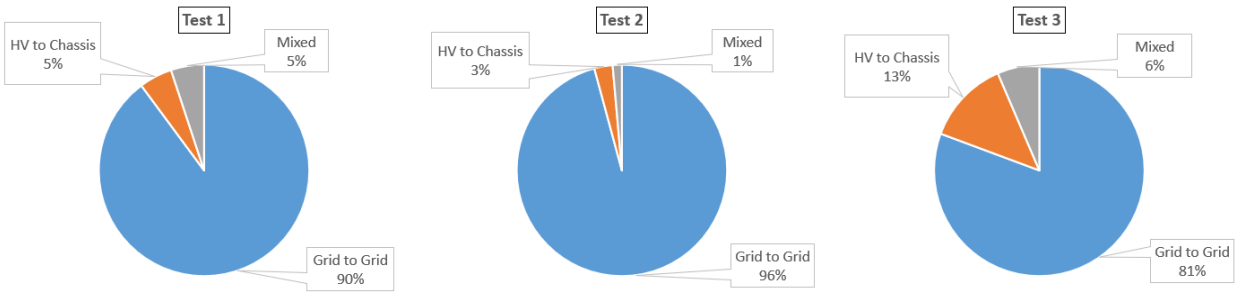

Figure 16: Arc type summary within the standard throttle table.

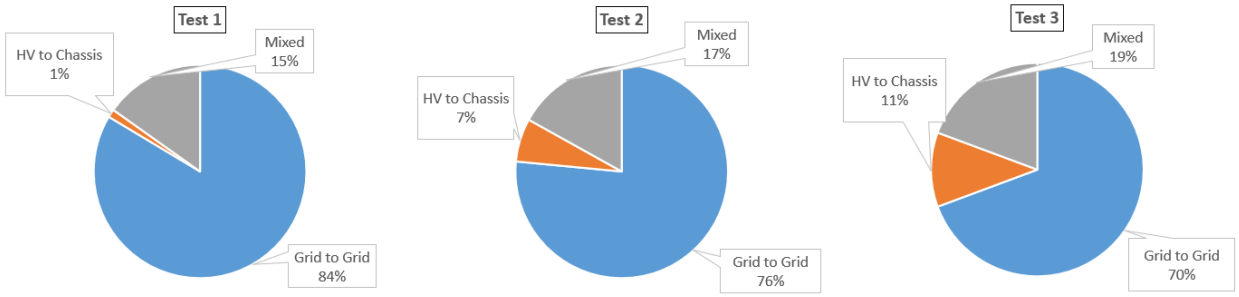

Figure 17: Arc type summary at the high thrust density conditions.

Discussion

The key results can be summarized as follows:

1. As anticipated, the majority of recycles were due to a grid-to-grid arcs. The proportion of high voltage-to-chassis arcs consistently increased with beam current across the three test segments, indicating that up to 30% of the recycles were consistent with high voltage-to-chassis arcs.

2. The chassis currents measured for high voltage-to-chassis arcs consistently ranged from 20 to 70 A for the tested hardware configuration. However, it was determined that more than 80% of the output current from the beam supply flowed through the neutralizer cathode plasma. In a flight configuration, the spacecraft chassis will act as the ground, and the available exposed surfaces will be more limited, so this particular result may be to be an artifact of the ground test configuration.

3. The recycle rate and arc type behaviors of the engine was influenced by the current density concentration and to a lesser extent by the magnitude of the beam current. While the baffle structure reduced the recycle rate by several orders of magnitude at the high thrust density conditions, it ultimately had little effect on the recycle type at elevated beam currents.

The data presented is specific to the hardware configuration and provides a baseline for distinguishing the type of arcs It shows that high voltage-to-chassis arcs account for a non-negligible percentage of total recycles, regardless of the hardware configuration, particularly under high thrust density conditions. Future work will include system integration tests with a prototype PPU and higher-fidelity thruster hardware, providing additional data on the factors that may influence recycling within the propulsion system. The next section outlines susceptibility tests that can be conducted to ensure proper integration of the propulsion system with the spacecraft.

Finally, when reviewing the data, it is important to note that the recycle rate observed during ground tests is typically several orders of magnitude higher than that demonstrated in flight. For example, each of the three NSTAR

engines on the Dawn mission only experienced a total of 40 - 70 recycles a piece during the first 20,000 hours of operation, with a significant portion of these arcs occurring during the initial engine firings [16]. The difference between ground and flight data can be attributed to several factors. Ground tests often utilize development grade hardware, which lack the iterative engineering improvements present in flight hardware. Furthermore, the ground hardware may undergo numerous atmospheric/vacuum cycles, leading to outgassing each time the thruster is retested under vacuum. Additionally, cryogenic facility regenerations during long duration wear tests have been found to influence the arc rate. Finally, the thrusters may also operate under highly off-nominal conditions while establishing flow and electrostatic margins, further impacting the frequency of arcs. As such, while the discussed recycle rates may align with previous ground test data, they do not accurately reflect in-flight performance.

VIII. Conducted Susceptibility Testing

The NEXT-C Power PPU accepts input power from the DART spacecraft Low Power Bus (LBP), nominally 30 V, and High-Power Bus (HPB), nominally 100 V. The PPU includes six interconnected DC-DC converters that create the isolated high-voltage and high-current supplies required to power the ion thruster. The LPB and HBP inputs to the PPU are isolated from chassis. The NEXT-C PPU exclusively uses isolated DC-DC converters, and the neutralizer common is used as a reference for the output power to the thruster. As with the previously discussed power console, the neutralizer cathode terminal at the PPU is connected to the PPU chassis, and consequently to the spacecraft chassis, through the following circuit elements:

1) Bi-directional Zener diode clamp: Back-to-back Zener diodes conduct if the neutralizer common potential exceeds the chassis potential by +/- 68V.

2) Ceramic capacitor: A capacitor connected between Neutralizer Common and chassis conducts current proportional to the time derivative of the voltage between neutralizer common and chassis (dV/dt).

3) Resistor: A resistor provides a DC connection between neutralizer common and chassis. This resistance has a negligible impact on high voltage breakdown behavior, so it will be ignored in this investigation.

Prior to a recycle event, the beam supply output capacitance is charged up to the beam voltage, which was nominally 1021 V for the DART operating condition, an 0.26 J energy source. When a thruster arc occurs, this capacitance can rapidly discharge, causing a transient current. During grid-to-grid recycles, this transient arc current is contained within the PPU-thruster system, and the transient current minimally involves the spacecraft chassis. However, a high-voltage-to-chassis arc that a portion of the transient current returns through the PPU's chassis connection. During this arc type, the capacitor conducts current proportional to the time derivative of the voltage between neutralizer common and chassis ($I = C*dV/dt$). When the neutralizer common to chassis voltage reaches approximately -68V, the PPU's parallel Zener diode conducts the fault current, clamping the voltage. This creates the possibility that thruster arc current flows in the spacecraft chassis to return to the PPU. Laboratory testing was performed on the NEXT-C PPU with a resistive load, using a mercury relay to simulate a high voltage-to-chassis fault. Figure 18 shows the PPU's chassis arc current, beam voltage, and neutralizer common to chassis voltage during a simulated high-voltage-to-chassis recycle. This test result is simplistic in that the thruster was simulated with a mercury relay, and the inductance of the cable harnesses were not necessarily flight-like. This test result is also conservative in that all of the high voltage-to-chassis arc current flows through Path 1 of Figure 9a and none through Path 2. However, it does illustrate that the PPU's stored energy will rapidly discharge in a RLC circuit.

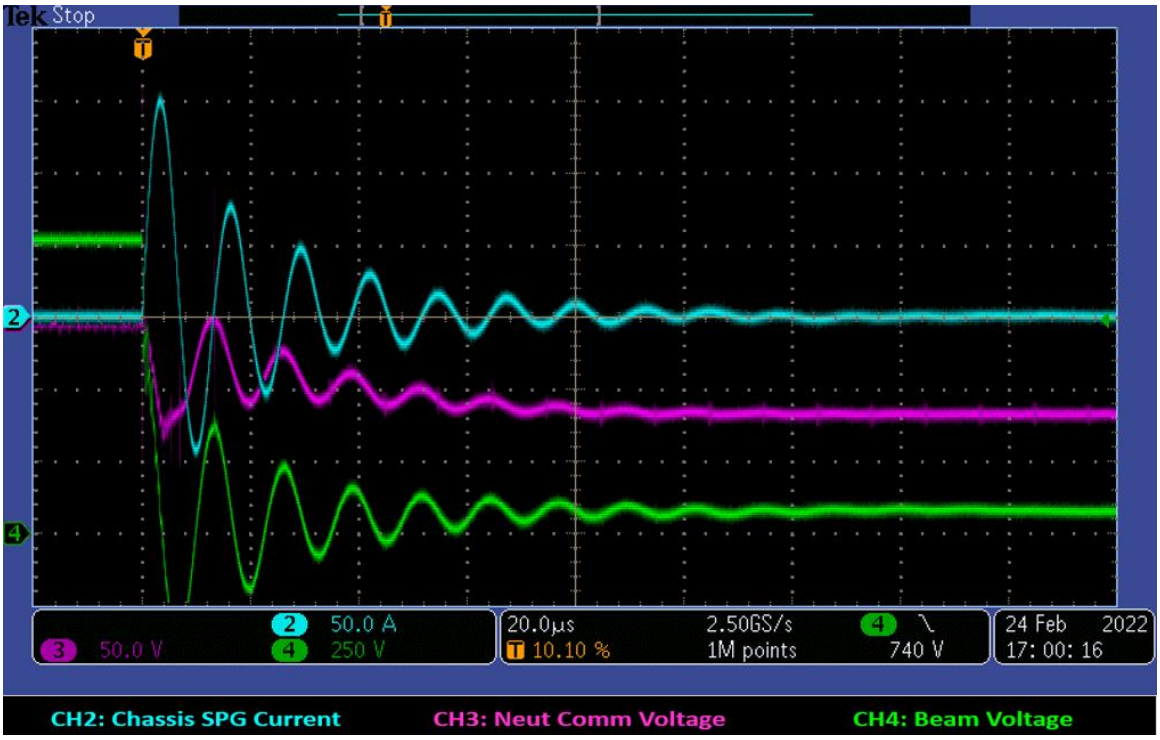

Figure 18: NEXT-C PPU laboratory test high-voltage to chassis recycle voltage and current waveforms.

As with any power system, the transient current will return in the lowest impedance (resistance plus inductive reactance) path. Therefore, careful spacecraft power system design can ensure that most of the fault current returns to the PPU on the PPU to thruster cable harness shield. However, under certain spacecraft bonding and grounding conditions, it is possible that a portion of the transient current returns through the spacecraft chassis. The NEXT-C team's recommendation is to add MIL-STD-461G conducted susceptibility test method CS116 to all hardware that operates on a spacecraft with an electric propulsion system like NEXT-C.

CS116: The CS116 test uses an inducer probe to inject damped sinusoid transients into the Unit Under Test (UUT). All signal and power cables are tested individually, with injection on the cable bundle, which drives common mode noise into the UUT. Additionally, all power cables must have their supply lines tested separately from their returns, which drives differential mode noise in the UUT. The damped sinusoids waveforms are shown in Figure 8. The damped sinusoids are tested at 10 kHz, 100 kHz, 1 MHz, 10 MHz, 30 MHz, and 100 MHz. The pulses are applied at a rate between 0.5 and 1 Hz for five minutes per test point. The peak current amplitudes for the test points are (10 kHz, 0.1A), (100 kHz, 1A), (1 MHz, 10A), (10 MHz, 10A), (30 MHz, 10A), and (100 MHz, 3A).

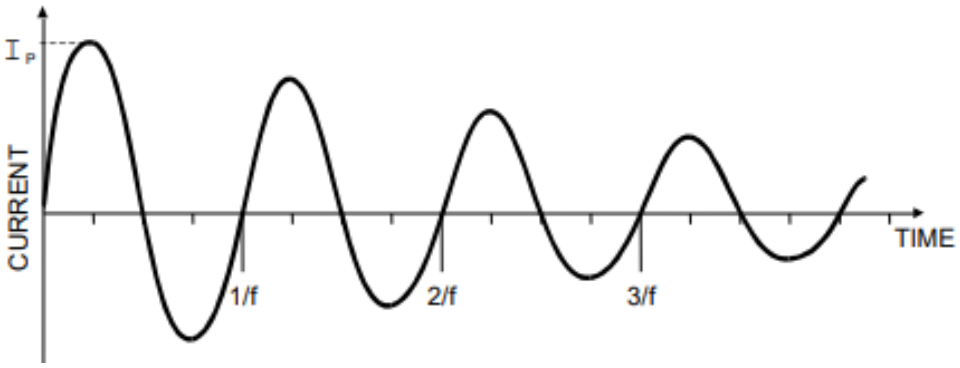

Figure 19: CS116 test waveform (MIL-STD-461G)

Note that the CS116 damped sinusoid waveform is similar to the chassis recycle current waveform observed in Figure 19, which was a damped sinusoid with approximate frequency of 83 kHz. The CS116 test setup attempts to simulate coupling to other harnesses as a result of this common mode disturbance and/or chassis ground bounce as this disturbance flows through the chassis impedance and creates a time variable voltage drop.

The CS116 MIL-STD-461G tests are performed on all interface cables, including both power and signal cables. Moreover, these tests use an inducer probe wrapped around the cable bundles to drive common mode currents into the device under test. This is a more realistic test as it mimics the type of common mode noise that the NEXT-C system could potentially to generate.

In summary, the NEXT-C team recommends that all missions that include gridded ion thrusters like NEXT-C must perform conducted susceptibility testing per CS116 per MIL-STD-461G. The importance of these MIL-STD-461G tests is that they are conducted on both signal cables and power cable, and that they inject common mode noise into the UUT. A CS116 test was conducted on the spare DART PSE hardware successfully replicated the in-flight anomaly.

The Advanced NEXT PPU adds a telemetry feature to determine whether a recycle was caused by a grid-to-grid arc or a high voltage-to-chassis arc. The NEXT-C PPU has a telemetry measurement on neutralizer common to chassis voltage. The Advanced NEXT PPU adds a peak detector circuit to the neutralizer common to chassis voltage measurement that is fast enough to capture the 10 μs spike to -68V. When the PPU detects a recycle, it checks the neutralizer common to chassis voltage peak voltage. If the peak voltage is more negative than a programmable threshold voltage, the PPU flags the recycle as a high voltage-to-chassis arc. If the peak voltage is more positive than the programmable threshold voltage, the PPU flags the recycle as a grid-to-grid arc. This circuitry will be tested during future system integration tests with the thruster and the prototype PPU.

IX. Summary

Test results from an engineering model Advanced NEXT thruster have been presented to identify various types of arcs observed with ground test hardware. Three distinct arc types were identified: grid-to-grid arcs, high voltage-to-chassis arcs, and a combination of both. The occurrence of recycles involving high voltage-to-chassis arcs varied between 4% and 30%, depending on the operating conditions and hardware configuration. Higher beam currents generally led to an increased frequency of high voltage-to-chassis arcs. During these arcs, chassis current levels ranged from 20-70 A, however, a substantial fraction of the current returned to the beam supply via the neutralizer cathode plasma, which may be a ground test effect. High voltage-to-chassis arcs were consistently observed, particularly under high-thrust-density conditions. Conducted susceptibility tests aimed at improving the integration of the propulsion system with the spacecraft have also been presented.

References

[1] Pinero, L.R. and Rawlin, V.K., "Recycle Requirements for NASA's 30 cm Xenon Ion Thruster," *30th AIAA/SAE/ASME/ASEE Joint Propulsion Conference*, AIAA-1994-3303, Indianapolis, IN, June 27-29, 1994.

[2] Rivkin, A.S., Cheng, A.F., "Planetary Defense with the Double Asteroid Redirection Test (DART) Mission and Prospects," *Nat Commun 14*, 1003, 2023.

[3] Fisher, J., et al., "NEXT-C Flight Ion System Status," *AIAA Propulsion and Energy 2020 Forum*, AIAA-2020-3604, August 24-28, 2020.

[4] Brophy, J.R., Garner, C.E., and Mikes, S.C., "Dawn Ion Propulsion System- Initial Checkout After Launch*," 44th AIAA/ASME/SAE/ASEE Joint Propulsion Conference*, AIAA-2008-4917, July 20-23, 2008, Hartford, CT.

[5] John, J., Roufberg, L., Ottman, G.K. and Adams, E., 2023, March. NEXT-C Lessons Learned on the DART Mission for Future Integration and Test. 2023 *IEEE Aerospace Conference*, pp. 1-7.

[6] Thomas, R.E., Pencil, E.J., Aubuchon, C.A., Goodfellow, K.D., Zubair, J.M., Bontempo, J.J., Bohurjak, M.A., Raju, R.S., and Patterson, M.J., "Development of the Advanced NEXT High thrust-to-power Gridded Ion System," *Joint Army Navy NASA Air Force Interagency Propulsion Committee*, Oklahoma City, OK, May 6-10, 2024.

[7] Shastry, R., Herman, D.A., Soulas, G.C., and Patterson, M.J., End-of-test Performance and Wear Characterization of NASA's Evolutionary Xenon Thruster (NEXT) Long-Duration Test," AIAA-2014-3617, *50th AIAA/ASME/SAE/ASEE Joint Propulsion Conference*, Cleveland, OH, July 28-30, 2014.

[8] Patterson, M.J., "NEXT Study of Thruster Extended-Performance (NEXT STEP)," *42nd AIAA/ASME/SAE/ASEE Joint Propulsion Conference & Exhibit*, AIAA 2006-4664, Sacramento, CA, July 9-12, 2006.

[9] Patterson, M.J., "NEXT Study of Thruster Extended-Performance II (NEXT STEP II)," *44th AIAA/ASME/SAE/ASEE Joint Propulsion Conference & Exhibit*, AIAA 2008-4808, Hartford, July 21-23, 2008.

[10] Patterson, M., Thomas, R., Arthur, N. and Crofton, M., "High Thrust-to-Power NEXT Thruster Assessment," *AIAA Propulsion and Energy 2019 Forum*, AIAA-2019-4022, Indianapolis, IN, August 19-22. 2019.

[11] Frandina, M.M., Arrington, L.A., Soulas, G.C., Hickman, T.A., Patterson, M.J., "Status of the NEXT Ion Thruster Long Duration Test," 41st AIAA/ASME/SAE/ASEE Joint Propulsion Conference & Exhibit, AIAA-2005-4065, Tucson, AZ, July 10-13, 2005.

[12] Pinero, L.R., Patterson, M.J., and Satterwhite, V.E., "Power Console Development for NASA's Electric Propulsion Outreach Program," 23rd International Electric Propulsion Conference, IEPC-93-250, Seattle, WA, Sept. 13-16, 1993.

[13] Soulas, G.C., Domonkos, M.T., and Patterson, M.J., "Performance Evaluation of the NEXT Ion Engine," *39th AIAA/ASME/SAE/ASEE Joint Propulsion Conference and Exhibit*, AIAA-2003-5278, Huntsville, AL, July 20-23, 2003.

[14] Shastry, R., and Soulas, G.C., "Post-test Examination of NASA's Evolutionary Xenon Thruster Long-Duration Test Hardware: Discharge Chamber," *52nd AIAA/SAE/ASEE Joint Propulsion Conference*, AIAA-2016-4630, Salt Lake City, UT, July 25-27, 2016.

[15] Hoskins, A., Wilson, F., Patterson, M., Soulas, G., Polaha, J., Talerico, L., and Sovey, J., "Development of a Prototype Model Ion Thruster for the NEXT System," AIAA-2004-4111, *40th AIAA/ASME/SAE/ASEE Joint Propulsion Conference & Exhibit*, July 11 - 14, 2004, Fort Lauderdale, FL.

[16] Garner, C.E., and Rayman, M.D., "In-Flight Operation of the Dawn Ion Propulsion System Through Completion of Dawn's Primary Mission," *52nd AIAA/SAE/ASEE Joint Propulsion Conference*, AIAA-2016-4539, Salt Lake City, UT, July 25-27, 2016.